Theor Ecol (2012) 5:387–401
DOI 10.1007/s12080-011-0131-3

ORIGINAL PAPER

Choice of density-dependent seedling recruitment function affects predicted transient dynamics: a case study with Platte thistle

Eric Alan Eager · Richard Rebarber · Brigitte Tenhumberg

Received: 13 October 2010 / Accepted: 11 May 2011 / Published online: 27 May 2011

Abstract Modelers have to make choices about which functional forms to use for representing model components, such as the relationship between the state of individuals and their vital rates. Even though these choices significantly influence model predictions, this type of structural uncertainty has been largely ignored in theoretical ecology. In this paper, we use integral projection models (IPMs) for Platte thistle as a case study to illustrate that the choice of functional form characterizing density dependence in seedling recruitment has important implications for predicting transient dynamics (short-term population dynamics following disturbances). In one case, the seedling recruitment function is modeled as a power function, and in the other case, we derive density dependence in seedling recruitment from biological first principles. We chose parameter values for the recruitment functions such that both IPMs predicted identical equilibrium population densities and both recruitment functions fit the empirical recruitment data sufficiently well. We find that the recovery from a transient attenuation, and the magnitude of transient amplification, can vary tremendously depending on which function is used to model density-dependent seedling recruitment. When we loosen the restriction of having identical equilibrium densities, model predictions not only differ in the short term but also in the long term. We derive some mathematical properties of the IPMs to explain why the short-term differences occur.

Keywords Transient dynamic · Density dependence · Integral projection model · Seedling recruitment function · Mechanistic modeling · Michaelis–Menten function

E. A. Eager (✉) · R. Rebarber
Department of Mathematics, University of Nebraska-Lincoln,
Lincoln, NE 68588, USA
e-mail: s-eeager1@math.unl.edu

B. Tenhumberg
School of Biological Sciences and Department of Mathematics,
University of Nebraska-Lincoln,
Lincoln, NE 68588, USA

Introduction

For structured population models, where members of the population are classified by one or more characteristic stages, most researches have been focused on analyzing long-term, asymptotic population characteristics, such as a population's asymptotic growth rate or equilibrium population density. However, when a population is forced away from its equilibrium stage distribution by disturbances such as environmental catastrophes or management actions, the subsequent dynamics of this population can change considerably in the short term (transient dynamics), making the analysis of such dynamics extremely relevant (Hastings 2004). For example, sudden changes in some vegetative distributions can significantly change the structure of associated animal communities (Snyder 2009; Weller and Spratcher 1965). The impacts of such disturbances on population dynamics can often not be elucidated with equilibrium analysis alone.

The majority of investigations of transients in discrete-time, structured population models have focused on models that are density independent (Caswell 2007, 2008; Koons et al. 2005; Tenhumberg et al. 2009; Townley et al. 2007; Townley and Hodgson 2008; Stott et al. 2010). However, many systems are driven by density-dependent mechanisms, but the signal for density dependence in empirical

data sets is often weak. A typical example of this is the seedling recruitment data of Rose et al. (2005, Fig. 1): the data are few, very noisy, and collected over a limited range of seed densities. It is challenging to find sensible functions that fit such noisy data well, and commonly used criteria to choose among different candidate functions such as Akaike information criterion (AIC) or Bayesian information criterion can only provide a relative ranking of "poor" fitting functions. Moreover, these statistical criteria do not consider the ability of a function to project dynamics outside the rage of observed data. This is particularly relevant if one is interested in dynamics outside the range of data collection, which is often the case when studying the effect of large perturbations that can cause transient dynamics. When projecting dynamics outside the range of data collected, we might consider functional forms that are derived from first principles, but do not rank first based on information criteria, and evaluate the effect of structural model uncertainty on model predictions.

In this paper, we use the *density-dependent* integral projection model (IPM) for Platte thistle (*Cirsium canescens*) developed by Rose et al. (2005) as a case study to evaluate the impact of structural model uncertainty on short-term behavior. Rose et al. (2005) represent density-dependent seedling recruitment with a power function of the form $f(x) = x^{\nu}$, where x is the density of seeds produced by the population in one time-step, $f(x)$ is the density of seedlings that result from these seeds and the parameter ν is fit to data. If $0 < \nu < 1$(which is essential to describe negative density-dependent dynamics), the power function has mathematical properties which include having an unbounded derivative for low seed densities and being unbounded for large seed densities. These extreme values of x are outside the range of seed densities considered in the statistical analysis of Rose et al. (2005). When studying transient dynamics, extreme values of x are highly relevant. Therefore, we derived an alternative function for seedling recruitment based on biological principles that takes into account these extreme values and ask the question: How sensitive are the predicted transient dynamics to the choice of the function used to characterize density-dependent seedling recruitment? Our alternative function describes seedling recruitment more realistically for extreme values of x, as recruitment is essentially linear for small seed densities and essentially constant for large seed densities. The resulting function is identical to the classical Michaelis–Menten, Beverton–Holt, or Holling type II functional response functions. We will call it the Michaelis–Menten function for the remainder of the paper.

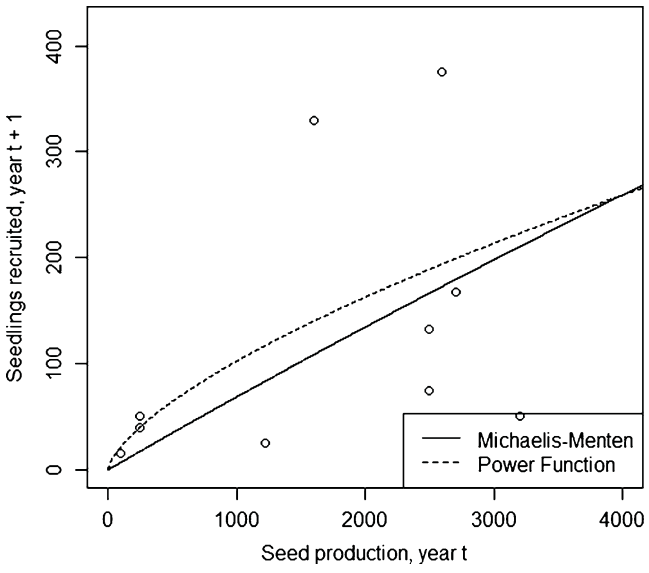

Fig. 1 The relationship between seedling recruitment in year t+1 and estimated seed production in year t. We digitized the data from Fig. 4 in Rose et al. (2005) and calculated the parameter ν in the power function to obtain an estimate of the AICc (AIC with a correction for finite sample sizes) value. Our estimate for the parameter ν (ν=0.654) deviates only by 2% from the one reported by Rose et al. (2005, ν=0.67); The AIC values of the power function from the digitized data (AICc= 138.4) and the Michaelis–Menten function (AICc=139.3) are similar. The *dotted* curve is the power function ($f_1(x) = x^{0.67}$) and the solid curve the Michaelis–Menten function $f_2(x) = 3,482x/(49,741 + x)$. In Appendix 1, we describe parameter estimation procedure of the Michaelis–Menten function

Other theoretical studies have emphasized that in many circumstances, statistically well-fitting nonlinear functions are not ecologically realistic (see, for instance, Cousens 1991; Freckleton et al. 2008; Runge and Johnson 2002). However, this paper highlights the role that the functional form of the density dependence plays in short-term, transient dynamics which, to our knowledge, has not been addressed.

To create a consistent setting for our derivation, we will first give a detailed account of the dimension of each function used in the IPM. We consider it desirable for a candidate recruitment function to have dimensions that are consistent with the rest of the IPM. We will then illustrate the differences in transient dynamics between the IPM using the power function and the Michaelis–Menten function by simulating two ecological events. The first simulation will mimic an ecological catastrophe, like a fire that destroys all above-ground plant biomass, where the initial population will consist entirely of seedlings (recruited from surviving seeds left in the ground). Second, we will simulate an ecological restoration project where the initial population consists of large, adult plants. We show that both IPMs can yield surprisingly large differences in transient dynamics even though the fit of the Michaelis–Menten function to the empirical data is comparable to the power function (Fig. 1) and both IPMs predict the same equilibrium population density. We derive mathematical properties of the two models that show why these differences occur and further verify these results after loosening

the restriction that the two models predict identical equilibrium population densities.

Model

Density-dependent integral projection model IPM for Platte thistle

An IPM can be used to describe how a population with a continuously varying stage structure changes in discrete time (Easterling et al. 2000). The use of IPMs in plant ecology has grown tremendously over the last decade (Ramula et al. 2009). See Briggs et al. (2010) for a tutorial on constructing IPMs. The population is characterized by a function, $n(x,t)$, where

$$\int_{x-\delta x}^{x+\delta x} n(y,t)\mathrm{d}y \tag{1}$$

gives the total density of the population near stage x and time t, with dimension plants(area)$^{-1}$. This function can be thought of as a continuous-stage analog to population vectors $n(t)$ in population projection matrix models (e.g., Caswell 2001). We have chosen to use an IPM because the ability to capture the transient dynamics is often linked to model dimension (the number of life history stages) (Tenhumberg et al. 2009; Stott et al. 2010). In a general IPM, the population $n(x,t)$ satisfies the integrodifference equation,

$$n(x,t+1) = \int_{L}^{U} K(x,y)n(y,t)\mathrm{d}y, \tag{2}$$

where $K(x,y)$ is called the kernel of the IPM and L and U are the smallest and largest observed value for the stage, respectively. We decompose the kernel into two parts:

$$K(x,y) = p_1(x,y) + p_2(x,y), \tag{3}$$

where $p_1(x,y)$ describes survival and growth, which models the probability of "movement" from stage y to stage x in one time-step. The "fecundity" portion of the kernel, $p_2(x,y)$, models the density of stage x individuals that are produced by stage y individuals.

We use a version of the model of Rose et al. (2005) that ignores the effect of seed predation (Briggs et al. 2010); this modification does not affect the way density dependence is implemented in the model. The natural logarithm of the plant's root crown diameter is used as an indicator of plant size (the stage variable); the time-step is 1 year. We start by mentioning the dimension of each of the model components to contrast the two seedling recruitment functions (Michaelis–Menten and power function) on the basis of dimensional analysis. The Platte thistle population's distribution, $n(x,t)$, has the dimension of plants(size)$^{-1}$(area)$^{-1}$. Let $s(y)$ and $f_p(y)$ be the survival and flowering probabilities, respectively, of members of the population with size y. If we call the growth function $g(x,y)$ where

$$\int_{x-\delta x}^{x+\delta x} g(z,y)\mathrm{d}x \tag{4}$$

is the probability of a size y plant growing to a size near x in one time-step (which is a probability distribution for each fixed y), then we have

$$p_1(x,y) = s(y)(1-f_p(y))g(x,y), \tag{5}$$

where the functions $s(y)$ and $f_p(y)$ are dimensionless, while $g(x,y)$ has the dimension of (size)$^{-1}$ (with $\int_{x-\delta x}^{x+\delta x} g(z,y)\mathrm{d}z$ being dimensionless).

The probability of not flowering, $1-f_p(y)$, is incorporated into the survival part of the kernel because Platte thistle is a monocarpic plant and, as a consequence, flowering is fatal. The model assumes that survival, flowering, and growth are independent events and that seedling size is independent of the size of the mother plant (a low maternal effect on seedling size has also been reported for other plant species (Weiner et al. 1997; Sletvold 2002)).

The fecundity portion of the kernel is

$$p_2(x,y) = p_e s(y) f_p(y) S_d(y) J(x), \tag{6}$$

where $S_d(y)$ is the number of seeds produced by members of the population with size y (with dimension of (seeds)(plant)$^{-1}$), and $J(x)$ is the probability distribution of the size of seedlings, with dimension of (size)$^{-1}$. The term p_e (with dimension of plants(seed)$^{-1}$) is the probability of a seed establishing to become a seedling by the next time-step, that is, the probability that a seed germinates and survives until the next population census. Seed establishment probability for Platte thistle is *density-dependent* (Rose et al. 2005). Thus, if $y(t)$ is the density of seeds produced by the population at time t, the seed establishment probability is given by

$$p_e(t) = \gamma(t)^{v-1}, \tag{7}$$

where the estimated value for v in Rose et al. (2005) is 0.67, which is the value we use in this paper. The function describing the size structure of seedlings, $J(x)$, is independent of y, and from the construction of the kernel, we see that the density of seeds produced is

$$\gamma(t) = \int_{L}^{U} s(y) f_p(y) S_d(y) n(y,t)\mathrm{d}y. \tag{8}$$

Thus, the full density-dependent IPM is

$$n(x,t+1) = \int_L^U p_1(x,y)n(y,t)\mathrm{d}y + \int_L^U \gamma(t)^{\nu-1}J(x)s(y)f_p(y)S(y)n(y,t)\mathrm{d}y. \quad (9)$$

More concisely,

$$n(x,t+1) = \int_L^U p_1(x,y)n(y,t)\mathrm{d}y + J(x)\gamma(t)^{\nu}. \quad (10)$$

Notice that the model in Eq. 10 is the sum of a density independent growth and survival and density-dependent seedling recruitment. We write a *general* seedling recruitment function as $f(\gamma(t)) = p_e(\gamma(t))\gamma(t)$, in order to stress that this function is the product of the seed establishment probability and the density of seeds at time t. When $p_e(\gamma(t))$ is as in Eq. 7, we have that $f(\gamma(t)) = \gamma(t)^{\nu} = p_e(\gamma(t))\gamma(t)$. We must note that some authors have used the term "recruitment" to mean the same as "establishment probability" (see, for instance, Runge and Johnson 2002). In this paper, these terms are used to describe two distinct, albeit related, concepts, as seedling recruitment is the product of seed establishment and seed density.

In general, a seedling recruitment function, $f(\gamma(t))$, has the dimension of plants(area)$^{-1}$, which is consistent dimensionally with the rest of the model. Hence, $p_e(\gamma(t))$has the dimension of plants(seed)$^{-1}$. Since $\nu \in (0,1)$, the function $p_e(\gamma(t)) = \gamma(t)^{\nu-1}$ does not have these dimensions for any choice of $\nu \in (0,1)$. In the next section, we derive a seedling recruitment function from first principles so that every parameter has a clear biological interpretation from the dimensional analysis point of view.

Derivation of seedling recruitment function

To mechanistically derive the seedling recruitment function, $f(\gamma(t))$, we follow in the spirit of the derivation of the Holling type II functional response in classical predation theory (Holling 1959). We envision seeds participating in "predation of space", with the analogy of "handling time" by Holling in classical predation theory becoming "handling space" in our derivation. In this model, we only consider *intraspecific* competition. In the "Discussion" section, we will talk about how to include *interspecific* competition in this framework.

Let $N(t)$ be the density of seedlings that are recruited between time t and $t+1$, i.e., the density of seeds produced that survive to become a seedling within one time-step. First, we make the assumption that the number of seedlings between time t and $t+1$ increases with the space available for seeds to establish, $S(t)$, which has the dimension of area. Also, assume that $N(t)$ increases (as a function of $\gamma(t)$) with the establishing efficiency rate a, where a has the dimension plants(seed)$^{-1}$(area)$^{-1}$. A first attempt at a relationship between $N(t)$ and $\gamma(t)$ yields

$$N(t) = aS(t)\gamma(t). \quad (11)$$

To obtain a more realistic relationship between $N(t)$ and $\gamma(t)$, it is reasonable to assume that the space available to establish will decrease with the number of seedlings, so $S(t)$ is decreasing with respect to $N(t)$. We envision a seed addition experiment where only seeds compete among themselves for the available microsite area. If we define the constant S_e to be the space taken up (as a proportion of the total space available) by one seed that establishes and becomes a seedling, where S_e has dimension area(plant)$^{-1}$, we can re-write $S(t)$ as follows:

$$S(t) = S_{\mathrm{tot}} - S_{\mathrm{tot}}S_eN(t) = S_{\mathrm{tot}}(1 - S_eN(t)), \quad (12)$$

Where S_{tot} is a fixed characteristic of the population's environment and is the total area of the space available for the plant population's seeds to establish. Substituting Eq. 12 into Eq. 11 and solving for $N(t)$ yields:

$$N(t) = \frac{aS_{\mathrm{tot}}\gamma(t)}{1 + aS_{\mathrm{tot}}S_e\gamma(t)}. \quad (13)$$

Or, more concisely,

$$N(t) = \frac{\alpha\gamma(t)}{\beta + \gamma(t)}, \quad (14)$$

where

$$\alpha = (S_e)^{-1}, \beta = (aS_{\mathrm{tot}}S_e)^{-1}. \quad (15)$$

The dimensions of α and β are plants(area)$^{-1}$ and seeds(area)$^{-1}$, respectively. Eq. 14 is the Michaelis–Menten function. Notice that, if we let $N(t)$=$f(\gamma(t))$, we can write

$$f(\gamma(t)) = \left(\frac{\alpha}{\beta + \gamma(t)}\right)\gamma(t) = p_e(\gamma(t))\gamma(t). \quad (16)$$

Using the Michaelis–Menten function for seedling recruitment, we can clearly interpret the parameters and their dimensions in a way that is consistent with the rest of the model. For example, the function $p_e(\gamma(t))$ has dimension of plants(seeds)$^{-1}$ and decreases to zero as the number of seeds grows to infinity, as one should expect in the dynamics of negative density-dependent seed establishment. Also, when $\gamma(t) \approx 0$, we see that $p_e(\gamma(t)) \approx \alpha(\beta^{-1}) = aS_{\mathrm{tot}}$, which describes the probability of a seed establishing in the total

absence of density dependence. β is an analog for the familiar half-saturation constant in classical predation theory (Vandermeer and Goldberg 2003) and is here the seed production needed to attain half of the maximum total seedling recruitment, α.

The Michaelis–Menten function is a limiting case of the derivation of a general seedling recruitment function of Duncan et al. (2009), which considers "safe sites" for seeds to establish and makes assumptions about the distribution of seeds after flowering and dispersal. The derivation in this paper is considerably simpler and, given that we are not modeling space explicitly as a variable in the population, perhaps more appropriate for this setting.

For the remainder of this paper, we call the IPM that uses the power function for seedling production the "power function" model, and we call the IPM that uses the Michaelis–Menten function the "mechanistic" model. Note that the survival, growth, seed production, and distribution of seedlings portions remain identical in the two models, and therefore, these names are simply to distinguish the way the seedling recruitment is implemented in the IPMs.

Results

To compare the two Platte thistle IPMs fairly, we initially calibrated the parameters of the Michaelis–Menten function to obtain the same equilibrium population density as the power function model (see Appendix 1). Therefore, the subsequent comparisons in Example 1a and 1b are of two IPMs having identical equilibrium population densities and size distributions. The fit of the calibrated Michaelis–Menten to the empirical recruitment data was comparable to the fit of the power function used in Rose et al. (2005) (see Fig. 1).

We define the transient function $T(t,\rho)$ to be the per-capita difference in the total population density from one time-step to another, dependent on the initial population distribution, $\rho(x)$. Mathematically,

$$T(t,\rho) := \frac{\|n(\cdot,t)\| - \|n(\cdot,t-1)\|}{\|n(\cdot,t-1)\|}, \quad t = 1,2,..., \tag{17}$$

where $\|\ \|$refers the L^1 norm defined by

$$\|\varphi(\cdot,t)\| := \int_L^U \varphi(x,t)\mathrm{d}x, \tag{18}$$

which equals the total population density of $\varphi(x,t)$, with dimension plants(area)$^{-1}$. This transient function definition is similar to the GR metric used in Koons et al. (2005) for matrix models and is a function of t and ρ alone, as $n(x,t)$ implicitly depends on the initial population ρ. The "$\cdot$" symbol indicates that the stage variable, x, is integrated away. This measurement of transients compares the population's current total density with its total density *in the previous time-step*. We say that the population experiences a *transient attenuation* at time t_0 if $T(t_0,\rho) < 0$and a *transient amplification* if $T(t_0,\rho) > 0$. Note that we can re-write the transient function as the per-capita growth rate minus unity. This makes clear our intention to have the cutoff between transient attenuation and amplification at zero. Therefore, using our definition, if a population has a transient attenuation (amplification), it has a smaller (larger) density than it had one time-step ago.

We have made certain to explicitly write that the transient function depends on the initial population distribution because the transient dynamics of a single-species, structured population tend to depend on the population structure that is remaining after the ecological disturbance corresponding to t=0. For examples of this phenomenon in density independent matrix models, see Townley et al. (2007) and Koons et al. (2005). Next, we illustrate that the stage structure of the initial population is the key determinant of the transient dynamics predicted by the Platte thistle IPMs and provide the proof in Appendix 2. For a non-zero population $n(x,t)$, which solves the density-dependent IPM

$$n(x,t+1) = \int_L^U p_1(x,y)n(y,t)\mathrm{d}y + f(\gamma(t))J(x), \quad n(x,0) = \rho(x), \tag{19}$$

the value of the transient function at time t_0+1 can be re-written as

$$T(t_0+1,\rho) = E_{n(\cdot,t_0)}((1-f_p(x))s(x)) - 1 + \frac{f(\|n(\cdot,t_0)\|E_{n(\cdot,t_0)}(c(x)))}{\|n(\cdot,t_0)\|}, \tag{20}$$

where $c(x) = s(x)f_p(x)S(x)$ and $E_{n(\cdot,j)}(z)$is the expected value of z subject to the probability density function defined by $P(x,j) := n(x,j)(\|n(\cdot,j)\|)^{-1}$. More specifically, the initial value of the transient function is

$$T(1,\rho) = E_{\rho(\cdot)}((1-f_p(x))s(x)) - 1 + \frac{f(\|\rho(\cdot)\|E_{\rho(\cdot)}(c(x)))}{\|\rho(\cdot)\|}. \tag{21}$$

This identity states that the transient function is the sum of expected probability of death (due to flowering and mortality) and expected per-capita seedling production. At equilibrium, the transient function is roughly zero, and therefore, per-capita seedling production offsets mortality. However, when a population is not at equilibrium, we can expect that the right-hand side of Eq. 20 will not be zero.

Note that the presence of the expected values in Eqs. 20 and 21 strengthens what is widely believed about the size distribution's impact on single-species transient dynamics. For example, in a plant population where the smallest plants have the lowest survival probability and produce the fewest seeds, one should expect that the largest transient attenuations would occur with an initial population largely consisting of small plants. This is due to the fact that the expected survival probability, seed production, and subsequent seedling recruitment for small plants will be small. This will result in the first term of the transient function plus the per-capita seedling recruitment being small relative to unity, resulting in negative transient function values.

A surprising result in this paper is that the total population density alone can explain why the predicted transient dynamics differ between the two models. For instance, if the population density in the power function model becomes sufficiently low (as in transient attenuation), the mathematical properties of the power function force the transient function to have extremely high values. Notice that in the power function model, the transient function can be re-written as:

$$T(t_0+1,\rho) = E_{n(\cdot,t_0)}((1-f_p(x))s(x)) - 1 + \frac{E_{n(\cdot,t_0)}(c(x))^{\nu}}{\|n(\cdot,t_0)\|^{1-\nu}}. \quad (22)$$

Assume that the initial population distribution is a predetermined density, M, of seedlings, i.e., $\rho(x) = MJ(x)$. In subsequent time-steps, the only *new members* of the population are seedlings, distributed according to $J(x)$. Because not all seedlings survive to their second year (for example, $E_{J(\cdot)}((1-f_p(x))s(x)) = 0.502$ in Rose et al. 2005) and grow to a much larger size, the stage distribution stays roughly the same for small t (see Eq. 10). Let us assume that the total population *density* changes in the right-hand side of Eq. 22 without changing the stage distribution at time t_0. This implies that the expected values in Eq. 22 are also unaffected. When $\nu \in (0,1)$, Eq. 22, viewed as a function of $\|n(\cdot,t_0)\|$, is *unbounded* as $\|n(\cdot,t_0)\|$ approaches zero. This is due to the fact that the derivative of the power function, $f'(x) = \nu x^{\nu-1}$, goes to infinity as x approaches zero. Thus, for every positive real number N, there exists a total population density $\|n(\cdot,t_0)\| = M_N$ such that for all total population densities *smaller* than M_N, we have

$$T(t_0+1,\rho) > N. \quad (23)$$

This conclusion in Eq. 23 states that, given a fixed stage distribution for the population, the power function model predicts that there exists a population density that ensures the beginning of a *recovery* (i.e., the population density starts rapidly increasing towards the equilibrium), once the total population density dips *below* this value. For instance, in the power function model, it is possible that a population of largely non-reproducing plants (seedlings) starts to grow once the population density drops below a particular threshold. We will illustrate this idea in Example 1a.

The previous mathematical artifact is not present in the mechanistic model, whose transient function can be written as

$$T(t_0+1,\rho) = E_{n(\cdot,t_0)}(1-f(x))E_{n(\cdot,t_0)}(s(x)) - 1 + \frac{\alpha E_{n(\cdot,t_0)}(c(x))}{\beta + \|n(\cdot,t_0)\|E_{n(\cdot,t_0)}(c(x))}. \quad (24)$$

When viewed as a function of $\|n(\cdot,t_0)\|$, Eq. 24 is a bounded function. Therefore, no threshold population density exists below which a population is guaranteed to increase. For instance, a population of seedlings cannot grow until some of the plants grow sufficiently large to reproduce.

When transient amplification occurs, the differences in the predictions of the two models stem from the properties of the two seedling recruitment functions when the seed production is greater than the equilibrium seed production $\gamma^* = \int_L^U s(y)f_p(y)S(y)n^*(y)\mathrm{d}y$ (here $n^*(y)$ is the equilibrium population). Because the power function $f(x) = x^{\nu}$ goes to infinity as x goes to infinity, in theory, the power function will eventually predict much larger seedling recruitment than the Michaelis–Menten function, and thus, everything else being equal, the power function model will have larger densities than the mechanistic model when seed production is large. In Example 1a and 1b, we chose model parameters so that equilibrium populations of the power function model and the mechanistic model are the same (see Appendix 1), thus

$$(\gamma^*)^{\nu} = \frac{\alpha\gamma^*}{\beta+\gamma^*}. \quad (25)$$

Assume that γ^* in Eq. 25 is the largest seed production such that the two seedling recruitment functions intersect (as it is the Example 1a and 1b, see Fig. 8). In a way that is analogous to the argument for transient attenuation, for any initial population $\rho(\cdot)$ and specified difference N between total population densities in the two models, there exists a seed production γ_N that elicits (at least) this difference at time t=1. To see this, let $n_1(\cdot,t)$ and $n_2(\cdot,t)$ and solve Eq. 19 with the same initial condition $\rho(\cdot)$, but with different seedling recruitment functions $f_1(\cdot)$ and $f_2(\cdot)$. Then, since the survival and growth portions of the kernel are the same for both models, one has

$$|(\|n_1(\cdot,1)\| - \|n_2(\cdot,1)\|)| = |f_1(\gamma(0) - f_2(\gamma(0))| \int_L^U J(y)\mathrm{d}y. \quad (26)$$

We then have that

$$|\|(n_1(\cdot,1)\| - \|n_2(\cdot,1)\|\| = |f_1(\gamma(0)) - f_2(\gamma(0))| \quad (27)$$

because $J(\cdot)$ is a probability distribution and the $f_i(\gamma(0))'s$ are independent of x. If $f_1(\cdot)$ is the power function, we have that if $\gamma(0) \to \infty$, it follows that $f_1(\gamma(0)) \to \infty$. In contrast, if $f_2(\cdot)$ is the Michaelis–Menten function, $\gamma(0) \to \infty$ implies that $f_2(\gamma(0)) \to \alpha$, which confirms the claim of the existence of a γ_N that elicits a difference of at least N between the two models. Furthermore, because

$$\gamma(0) = \|\rho(\cdot)\| E_{\rho(\cdot)}(c(x)), \quad (28)$$

it follows that, given an initial probability density function for the population, one can find $\|\rho(\cdot)\|_N$ such that for $\|\rho(\cdot)\| > \|\rho(\cdot)\|_N$, we have

$$\|n_1(\cdot,1)\| - \|n_2(\cdot,1)\| > N. \quad (29)$$

In Example 1b, we will assume a homogeneous initial population and display this result by showing how increasing $\|\rho(\cdot)\|$ increases the difference between the predicted populations after only one time-step.

Example 1a: transient attenuation

To illustrate the consequences of the preceding mathematical discussions for predicted transient dynamics, we first envision a brief ecological disturbance, like a fire, that wipes out the entire population of plants, with the exception of seeds in the soil that germinate to become seedlings in the following year, but does not significantly alter the long-term environmental conditions. While this is clearly an oversimplification, the goal of this example is to merely evaluate if the way we implement density dependence influences predicted transient dynamics.

To simulate this event, we will let $\rho(x) = MJ(x)$ be the initial population, which consists entirely of seedlings, so $\rho(x)$ is the population distribution of M seedlings(area)$^{-1}$. Very small plants do not reproduce, and seed production increases with plant size (see Rose et al. 2005), but plants of all sizes can die. Thus, we expect that a population consisting entirely of seedlings will decrease initially, before rising back to its equilibrium population density. Accordingly, for small t both IPMs predict transient attenuation because $c(x)$ is increasing and survival and the probability of not flowering are always below unity.

The main difference in transient dynamics between the two models is how quickly the population increases to its equilibrium density following the disturbance event (equal to speed of recovery from transient attenuation). We began our simulations with M values equal to 10, 15, 25, and 50 seedlings(area)$^{-1}$ using identical initial size distributions of the seedlings, $J(x)$ in each simulation. As expected, in both IPMs, the population density values decline initially (see t=1 in Fig. 2). However, the power function model predicts a faster recovery than the mechanistic model and the smaller the M value the larger is the difference between the predicted recovery patterns For example, if M=10 and t=10, the power function model predicts a population that is 4.75 times larger than that of the mechanistic model. This is in accordance with the mathematical observation in Eq. 23. Initially, the total population densities and size distributions of the populations are very similar for both models. However, when the population density becomes small enough, the transient function of the power function model has large positive values (relative to the mechanistic model), and faster recovery begins (see t=1 years in Fig. 3).

Example 1b: transient amplification

We expect transient amplification when the initial size distribution is skewed toward larger plants with higher reproductive value relative to the stable size distribution because the seed production $c(x)$ is increasing. We envision a restoration scenario where plants are grown in a greenhouse, until they reach a large target size and then transplanted into the field. In this case, the initial population consists entirely of large plants. To simulate this hypothetical situation, we used an approximation to the Dirac Delta distribution (an explanation of the Dirac Delta distribution can be found in Appendix 3), centered at nine tenths of U, the largest root crown diameter in the population. Thus, $\rho(x) = M\delta(x - 0.9U)$, with initial population densities, M, of 10, 15, 25, and 50. As Fig. 4 illustrates, the power function model predicts transient amplifications that are much larger relative to the mechanistic model, and this difference is more extreme for large initial population densities. If recruitment is modeled by the power function, the large seed densities produced by a population of large plants correspond to larger seedling densities compared to recruitment being modeled by the Michaelis–Menten function. This difference grows with the initial density because, naturally, large initial populations of seed-producing plants correspond to large seed production values, and thus, when large seed production values are the input for an *unbounded* power function, the model subsequently predicts larger seedling densities than that if we used the (bounded) Michaelis–Menten function. For example, in our simulation, a density of 50 large plants(area)$^{-1}$ produces 1,021,754 seeds. This is larger than the equilibrium seed production of γ^*=111,398 seeds (see Appendix 1 for this calculation), and thus, we would expect from Eq. 29 that the differences in recruitment would be quite large. In fact, the power function allows 1.03% of these seeds to become seedlings while the Michaelis–Menten function allows only 0.32% of these seeds to become seedlings. This difference in seed establishment

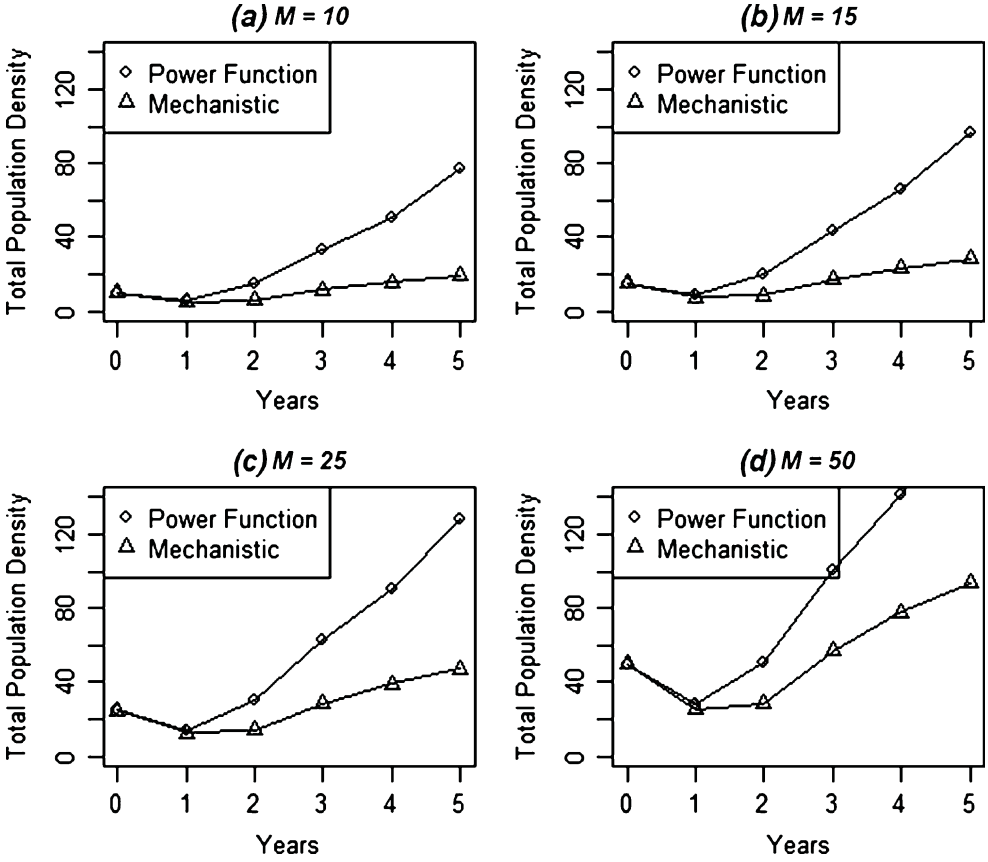

Fig. 2 Predicted transient population dynamics for the two Platte thistle models resulting from simulating the ecological event in Example 1a. The initial densities, *M*, are **a** 10, **b** 15, **c** 25, and **d** 50 seedlings/area; in each simulation, the size distribution of the seedlings was identical to that reported in Rose et al. (2005)

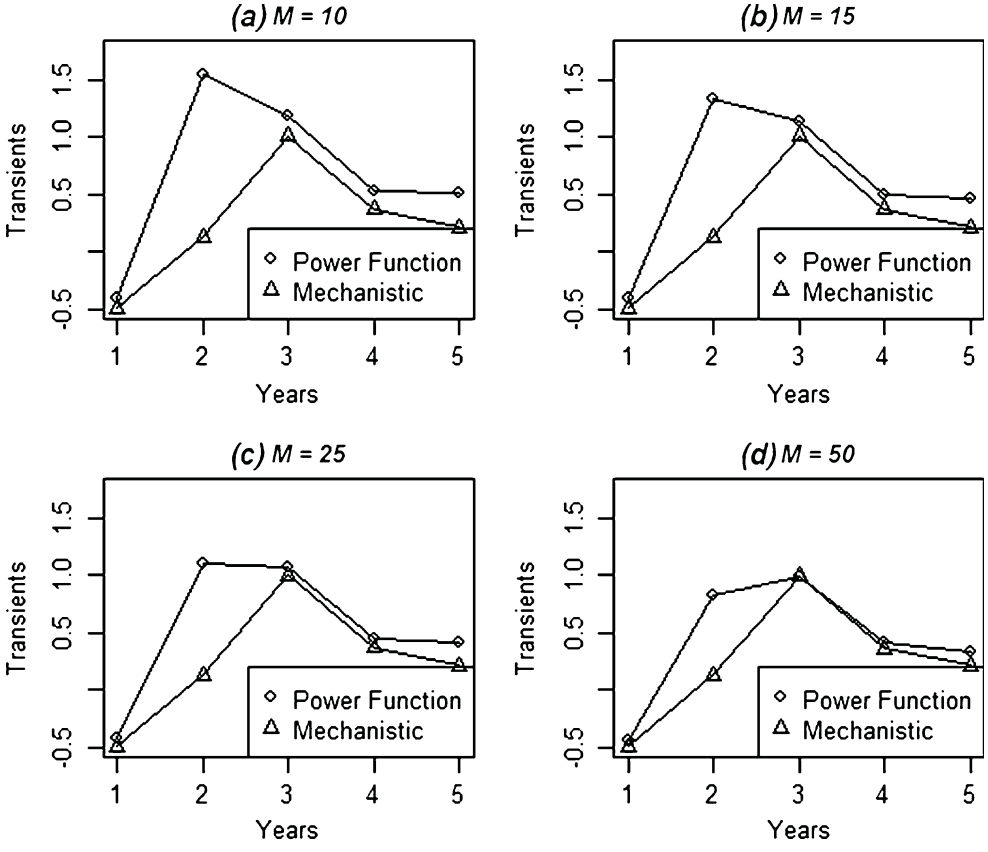

Fig. 3 Predicted transient function values for the two Platte thistle models resulting from simulating the ecological event in Example 1b. The initial densities, M, are (**a**) 10 (**b**) 15 (**c**) 25 and (**d**) 50 seedlings/area; in each simulation, the size distribution of the seedlings was identical to that reported in Rose et al. (2005)

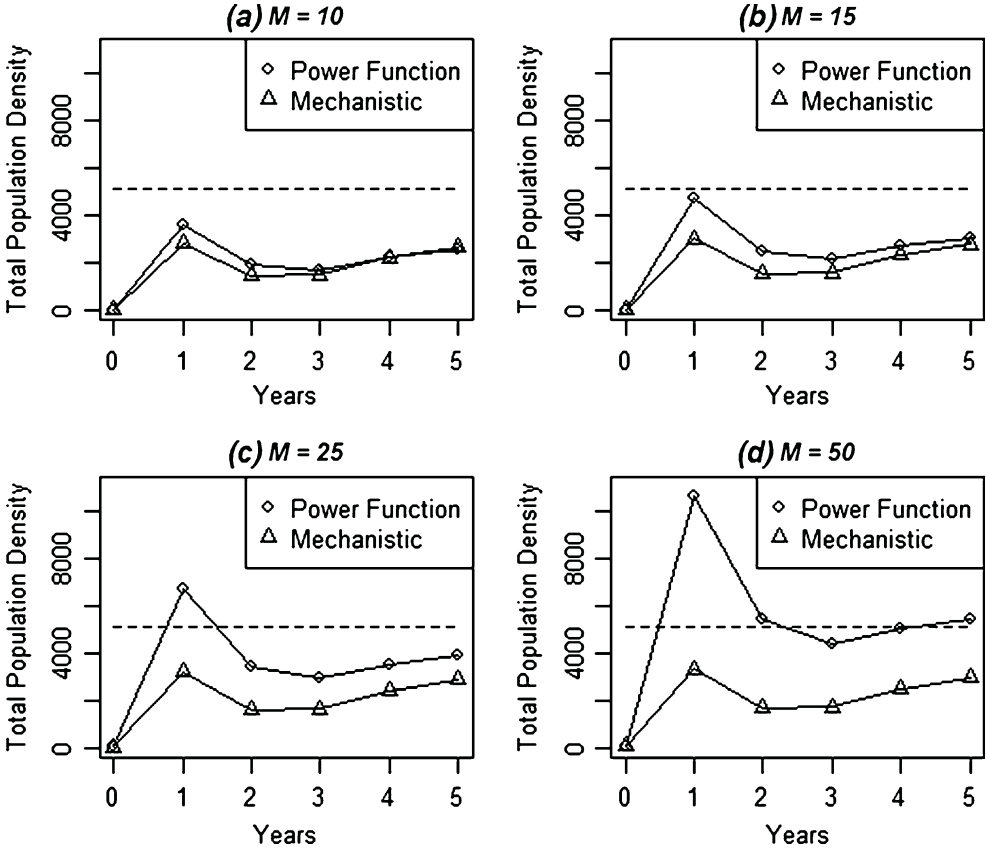

Fig. 4 Predicted total population densities for the two Platte thistle models resulting from simulating the ecological event in Example 1b. The initial densities, M, are **a** 10, **b** 15, **c** 25, and **d** 50; in each simulation, M was distributed according to the Dirac Delta distribution centered at nine tenths of the largest observable plant's size. The *dashed line* illustrates the equilibrium population density (~5,082 plants/area). For more on the Dirac Delta distribution, see Appendix 3

probability corresponds to an order-of-magnitude difference in transient amplification between the two models.

Example 2a: transient attenuation in models without identical equilibrium populations

Ecologists do not know the equilibrium population density; thus, when deciding which function best describes density-dependent seedling recruitment given the data, ecologists will independently estimate both parameters of the Michaelis–Menten function, rather than attempting to estimate the parameters to obtain a desired equilibrium. This approach produces differences in predicting the equilibrium dynamics and magnifies the difference in the short-term dynamics compared to the models with forced equal equilibriums. So, for this example, we used nonlinear regression analysis in R (R Core Development Team 2006) to estimate both model parameters from the data in Rose et al. (2005). Interestingly, this revised Michaelis–Menten function (which we will call the revised Michaelis–Menten function) predicts a much smaller saturation constant α (see Fig. 5). This yields a much smaller equilibrium seed production γ^* and, consequently, a smaller equilibrium population density ($\|n^*\| \approx 429$ plants(area)$^{-1}$). Since the revised equilibrium density is much closer numerically to the density at $t=0$ in simulations with similar initial conditions to Example 1a, the

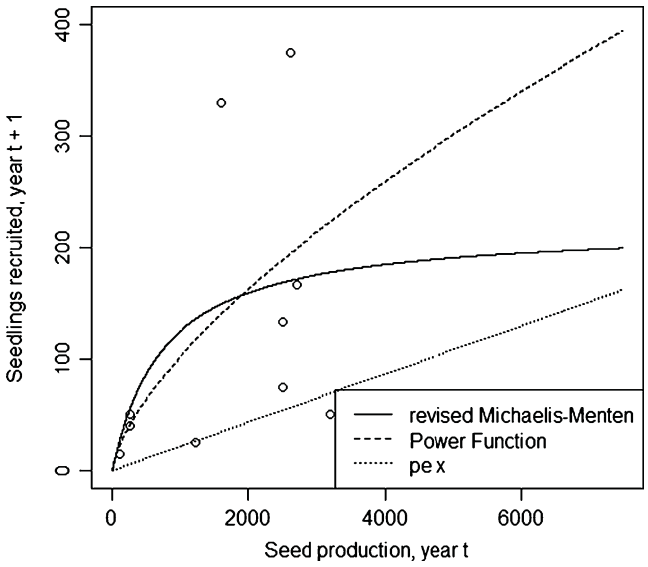

Fig. 5 The relationship between seedling recruitment in year $t+1$ and estimated seed production in year t. The *dotted* curve remains the power function $f_1(x) = x^{0.67}$ as in Rose et al. (2005) and the solid curve the revised Michaelis–Menten function fitted independently $f_2(x) = \frac{219.6x}{756.7+x}$. Note that the revised Michaelis–Menten function appears to be approaching its asymptote closer to the range of observable seed production. The AICc value for the revised Michaelis–Menten function (AICc=140.6) is very similar to that of the power function of the digitized data in Rose et al. (2005) (AICc=138.4) and the original Michaelis–Menten (AICc=139.3) function used in Example 1a and 1b

revised mechanistic model will converge to its equilibrium population density much faster. However, the mathematical observation in Eq. 23 about the transient function still holds, as when the initial population becomes smaller the difference between $T(1,\rho)$ in the two models grows (Fig. 6).

Example 2b: transient amplification in models without identical equilibrium populations

We used similar initial conditions as in Example 1b to compare the transient amplifications of the two models. Allowing for different equilibrium population densities produces larger differences in the short-term dynamics between the power function model and the revised mechanistic model compared to the previous models that forced the same equilibrium dynamics (Fig. 7). As Eq. 29 suggests, the population density in the power function model can get very large in one time-step (relative to the revised mechanistic model) due to the lack of a restrictive upper bound. In contrast, the revised Michaelis–Menten function has a relatively low saturation constant, and the equilibrium population recruitment is at saturation level, i.e, $\frac{\alpha\gamma^*}{\beta+\gamma^*} \approx \alpha$. This is because the straight line $h(\gamma) = p_e^*(\gamma)$ intersects the revised Michaelis–Menten function well into its asymptote (see Appendix 1). This means that the total population density at $t+1$ cannot grow larger than the total population density at t plus the maximum seedling recruitment α, and therefore, population trajectories from the revised mechanistic model remain relatively constant.

Discussion

Using Platte thistle as a case study, we have shown that the predicted transient dynamics can vary considerably depending on how we implement density dependence in recruitment, even if the equilibrium dynamics are the same. We have also shown that that these differences occur in models where the parameters are fit independently. Through mathematical arguments we verify that these differences in transient dynamics between these two models are due to the differences in functional form, and not simply a product of parameter uncertainty, as the results in Eq. 23 and Eq. 29 are for general power functions and general Michaelis–Menten functions. So while some parameter values may display these differences more drastically than others, the results in this paper suggest that for some ecological outcomes the predicted transient dynamics will differ, regardless of parameter values used, and these differences do not have a bound.

It is interesting to note that when the parameters in the Michaelis–Menten function were fit independently, the resulting equilibrium population density ($\|n^*\| \approx$ 429 plants(area)$^{-1}$) was similar to the beginning population

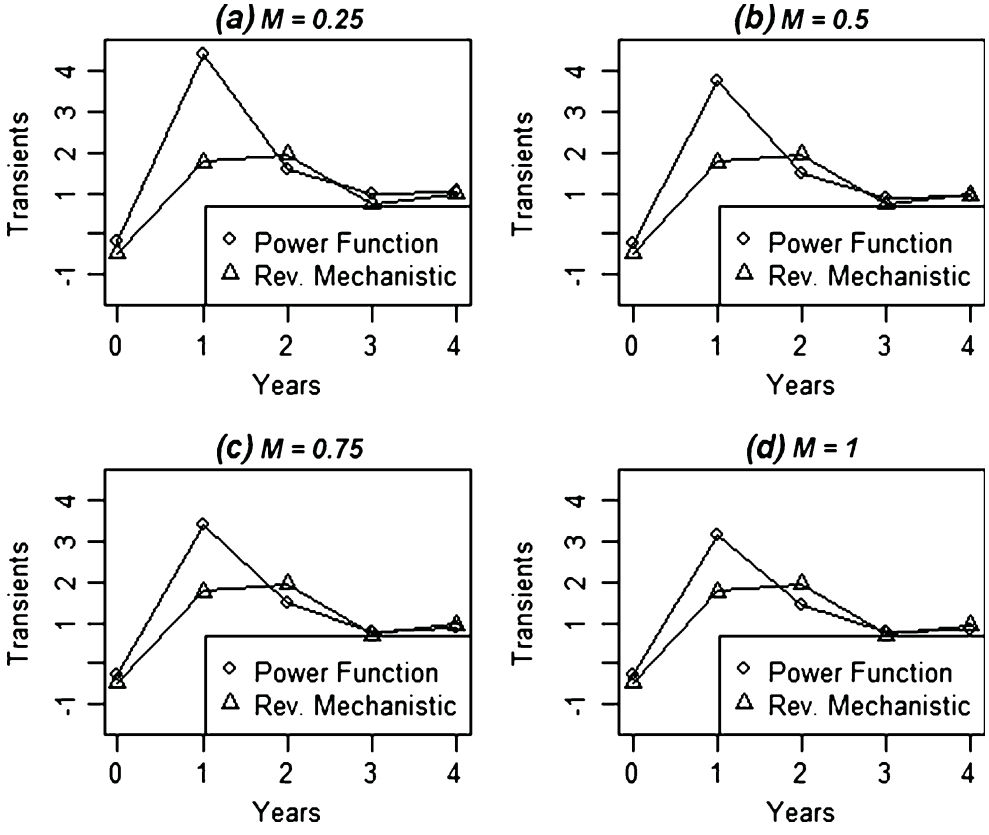

Fig. 6 Predicted transient function values for the power function model and the revised mechanistic model resulting from simulating the ecological event in Example 2a. The initial densities, M, are **a** 0.25, **b** 0.5, **c** 0.75, and **d** 1 seedlings/area; in each simulation, the size distribution of the seedlings was identical to that reported in Rose et al. (2005)

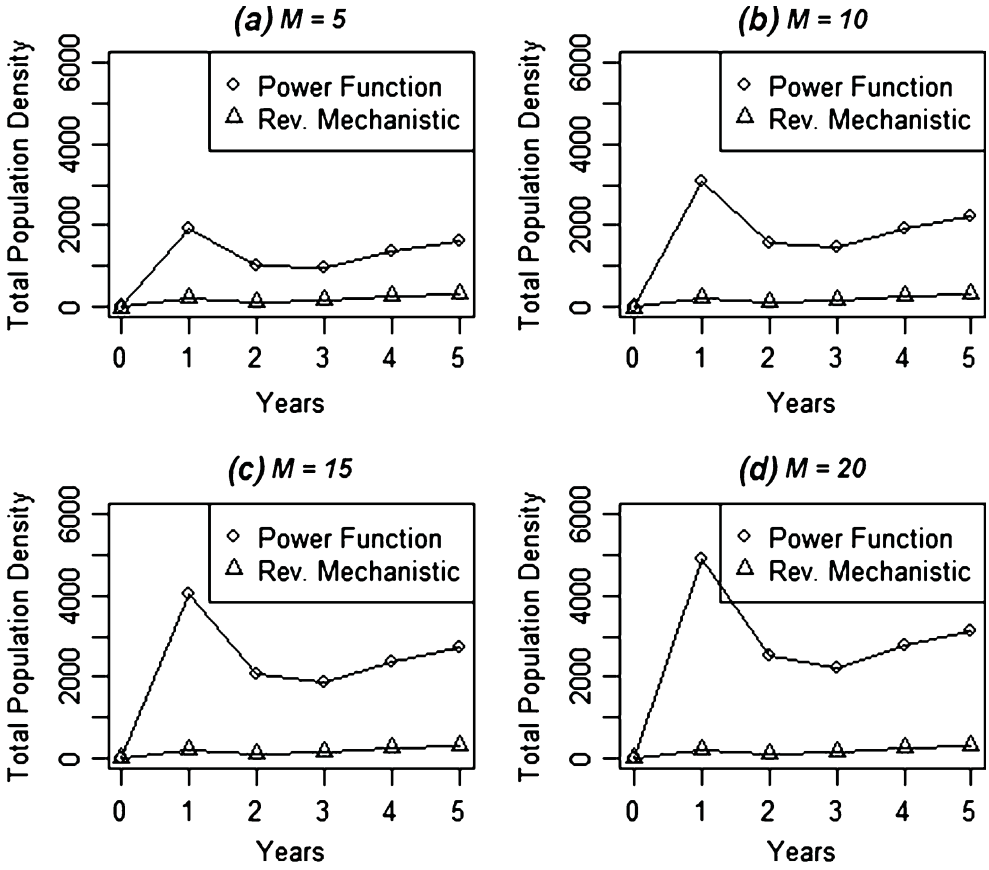

Fig. 7 Predicted total population densities for the power function model and the revised mechanistic model resulting from simulating the ecological event in Example 2b. The initial densities, M, are **a** 5, **b** 10, **c** 15, and **d** 20; in each simulation, M was distributed according to the Dirac Delta distribution centered at nine tenths of the largest observable plant's size

size reported in Fig. 1a in Rose et al. (2005) prior to the invasion by *Rhinocyllus*. This would appear to build on the suggestion made in this paper that mechanistic modeling, followed by standard methods of parameter estimation, offers the ideal prospect for obtaining a useful model when the data are poor.

The importance of choosing the most appropriate functional form for density-dependent recruitment has been recognized in other contexts. For example, Runge and Johnson (2002) have shown that the functional form used for recruitment can influence the optimal harvesting strategy for duck populations in a nontrivial way. They argue that the differences between these functions often lie outside the range of observed, or even anticipated, data, and therefore, statistical methods are limited in determining what functional relationships in vital rates are most appropriate. To address the effect of the resulting structural uncertainty on model predictions, the authors advocate for *active probing* of models that vary in their implementation of vital rates, which means exploring model predictions outside the realm of data collection. The benefit of this active scrutiny is often overlooked because "model validation" typically focuses on replicating *previously observed phenomena* (Maki and Thompson 2006). In the study by Rose et al. (2005), there were no empirical recruitment data for very low or very high seed densities available and the two alternative recruitment functions differ mainly in the unobserved data range (Fig. 1). The sensitivity of the predicted transient dynamics to the choice of the recruitment function highlights the value of active probing of model components.

Density dependence occurs due to the regulatory nature of limited resources in a system. The strength of density dependence should be highest at some carrying capacity, and population growth should not be limited at low population density, resulting in essentially linear dynamics. The Michaelis–Menten function is essentially linear for small seed densities (provided that β is sufficiently large). This implies that the density dependence does not influence population dynamics until the seed density is sufficiently high, which is what we expect to see. In contrast, when using the power function, seedling recruitment is never linear for low seed densities. Thus, the power function may poorly predict the dynamics at low density levels. In other words, while the population might not be experiencing the biological effects of density dependence, we are still predicting its dynamics subject to the *mathematical* effects of density dependence (Hastings 2004). In Example 1a, we discovered that the power function model's transient function can become arbitrarily large when the population's density becomes sufficiently small (Eq. 23). This is due to the fact that the power function's derivative is unbounded

for seed production densities close to zero, which causes seed establishment *probability* to be greater than unity for small seed densities. For example, if $\gamma(t)$=0.75, then

$$\gamma(t)^{\nu} = (0.75)^{0.67} = 0.82, \tag{30}$$

which implies that $p_e(t)$=1.09, which is clearly false, as seed establishment probability needs to be bounded above by a number smaller than unity to make sense. The *largest* seed establishment value for the Michaelis–Menten function is much smaller than unity, as $p_e(\cdot) \leq \alpha\beta^{-1} = 0.07$.

In the case where the total seed production is much larger than the available number of microsites, a constant number of seedlings are recruited for each time-step. No such limiting value will be obtained in the power function because it is unbounded for large seed values, and the number of seedlings always increases with the number of seeds produced. Even though models using the power function to represent density-dependent recruitment predict equilibrium population densities, the lack of an upper bound for recruitment may still lead to poor predictions of annual seedling recruitment if populations are skewed toward individuals with high reproductive value. The result is an overestimation of the potential magnitude of transient amplification (Eq. 29, Figs. 4 and 7). In contrast, the Michaelis–Menten function is more realistic in this situation because as the number of seeds produced goes to infinity, the density of recruited seedlings approaches the constant α. This constant is determined by the number of available microsites.

Apart from being more realistic, deriving functional relationships from first principles allows us to incorporate other relevant ecological mechanisms such as interspecific competition for limited microsites. In the presence of interspecific competition, density dependence would intensify and the maximum recruitment density would be lower. We can expand our derivation of the Michaelis–Menten function and insert a term for interspecific competition. If we let the aggregate seed density of other species competing with Platte thistle be denoted by $\omega(t)$, then our Michaelis–Menten function would have the form (Mangel 2006):

$$f(\gamma(t), \omega(t)) = \frac{\alpha\gamma(t)}{\beta + \gamma(t) + \omega(t)}. \tag{31}$$

This function has similar properties of the Michaelis–Menten function for seedling recruitment, that is, $f(\gamma(t), \omega(t))$is close to linear for low $\gamma(t) + \omega(t)$values and is roughly constant if $\gamma(t)$ becomes large. One additional property of $f(\gamma(t), \omega(t))$ is that it becomes small if $\omega(t)$ becomes large because all microsites are occupied by the competing species. In contrast, the power function has no similar, intuitive extension for incorporating interspecific competition.

We have shown that the choice of the functional forms such as density-dependent recruitment can have profound effects on predicted transient dynamics. This suggests that more emphasis should be placed on functional relationships that are derived based on mechanistic ecological principles.

Acknowledgments The authors would like to thank Bo Deng for suggesting that we derive the Michaelis–Menten function from first principles in the early stages of this work. We would also like to thank Haridas Chirakkal, Sara Reynolds, Mark Lewis, and another anonymous reviewer for their helpful comments on earlier drafts of this paper. Richard Rebarber was supported in part by NSF Grant 0606857.

Appendix 1: Calculating parameters to ensure common equilibrium values

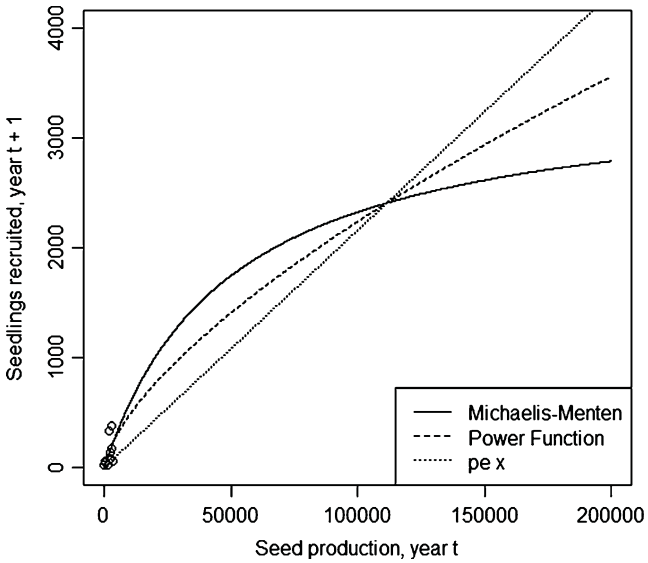

Fig. 8 The relationship between seedling recruitment in year t+1 and estimated seed production in year t. The intersection of the two recruitment functions with $h(x) = p_e^* x$ elicits the equilibrium seed production γ^*. We used this intersection to find the equilibrium population density (see Appendix 1). Note that the equilibrium seed production is much larger than the observed data in Rose et al. (2005), which are indicated by the *dots* near the origin

This section demonstrates how to find the parameter values for the seedling recruitment function in the mechanistic model that ensures that the power function and mechanistic model have a common equilibrium population. For our particular model, Rebarber et al. (2011) ensure that this equilibrium population exists for Eq. 19 and is globally stable, independent of non-zero initial population. To find this equilibrium population, we begin by writing Eq. 19 in abstract form. To do this, we define the bounded operator

$A_0 : L^1(L,U) \to L^1(L,U)$, the bounded functional $c^T : L^1(L,U) \to \Re$, and the $L^1(L,U)$ vector b by

$$A_0 u = \int_L^U p_1(\cdot,x)u(x)\mathrm{d}x, \quad c^T u = \int_L^U c(x)u(x)\mathrm{d}x, \quad b = J(x). \tag{32}$$

In this abstraction, A_0 is the survival/growth operator, c^T is the reproductive functional, and b is the distribution of newborns. We can now write our model as

$$\begin{aligned} n(x,t+1) &= A_0 n(x,t) + bf(c^T n(x,t)) \\ &= A_0 n(x,t) + p_e(c^T n(x,t))bc^T n(x,t). \end{aligned} \tag{33}$$

To calculate the equilibrium population, we first need the concept of the stability radius of the real, positive system(A_0, b, c^T). This is the smallest positive number p_e* such that the spectral radius of the operator $A_0 + p_e{}^* bc^T$ is equal to unity. It is proved in Hinrichsen and Pritchard (2005) that p_e* is given by the formula

$$p_e{}^* = (c^T(I - A_0)^{-1}b)^{-1}. \tag{34}$$

Suppose that f is increasing, concave down and $f(0)=0$, and let γ* be the solution of the equation

$$p_e{}^* = p_e(\gamma). \tag{35}$$

It is shown in Rebarber et al. (2011) that the equilibrium population is given by the formula

$$n^*(x) = (p_e{}^* \gamma^*)(I - A_0)^{-1}b, \tag{36}$$

and that γ* is the limiting seed production. Using the kernel functions in Table 2 of Rose et al. (2005), we compute that p_e*=0.0216, which we note, is independent of the choice of seedling recruitment function $f(\gamma(t)) = p_e(\gamma(t))\gamma(t)$. To find the limiting seed production, γ*, for both models, we solve Eq. 35. *This equality is what we need to match in the two seedling recruitment functions to obtain identical equilibrium populations*. For the power function model, Eq. 35 becomes

$$(\gamma^*)^{-0.33} = 0.0216, \tag{37}$$

from which we obtain γ*=111,397.68. To match the mechanistic model, we need to choose parameter values α and β in the Michaelis–Menten function in Eq. 14 such that p_e* = $p_e(\gamma^*)$, where γ*=111,397.68 and p_e*=0.0216. The Michaelis–Menten function has two parameters, which will allow us to use one parameter to ensure that $\alpha(\beta + \gamma^*)^{-1} = p_e{}^*$, with one additional parameter left to fit the empirical recruitment data in Fig. 4 of Rose et al. (2005). In this paper, we will allow β to be the free parameter, to be fitted to data, and solve for α in terms of β to obtain the common equilibrium population. In particular, $\alpha = 0.0216(111,397.68 + \beta)$. Finally, we used nonlinear regression to obtain β=49,741 from the data from Fig. 4 of Rose et al. (Fig. 1).

The calculation of p_e* and all other simulations of the IPMs in this paper use the numerical integration techniques described in Ellner and Rees (2006). All numerical techniques in this paper were carried out using the statistical software R (R Development Core Team 2006), and codes are available upon request.

Appendix 2: Proof of the identity in equation Eq. 18

To prove the identity in Eq. 20, we must first explicitly write the definition for the transient function at time t_0+1 with a given initial population $\rho(x)$. By the definition of $p_1(x,y)$ in Eq. 5 and $P(y,t_0) := n(y,t_0)(\|n(\cdot,t_0)\|)^{-1}$, we have

$$T(t_0+1,\rho) = \frac{\left\| \int_L^U p_1(\cdot,y)n(y,t_0)\mathrm{d}y + f(\gamma(t))J(\cdot) \right\| - \|n(\cdot,t_0)\|}{\|n(\cdot,t_0)\|} \tag{38}$$

$$= \int_L^U \int_L^U s(y)(1-f_p(y))g(x,y)P(y,t_0)\mathrm{d}y\mathrm{d}x + \frac{f(\gamma(t))}{\|n(\cdot,t_0)\|}\int_L^U J(x)\mathrm{d}x - 1 \tag{39}$$

$$= \int_L^U \int_L^U s(y)(1-f_p(y))g(x,y)P(y,t_0)\mathrm{d}y\mathrm{d}x + \frac{f(\gamma(t))}{\|n(\cdot,t_0)\|} - 1, \tag{40}$$

as the integral of the probability density function $J(x)$ is equal to unity. Since we are assuming that the functions in the kernel are all positive, sufficiently smooth functions, with $f_p(y) < 1$ for every y, we can use the Fubini–Tonelli Theorem (Folland 1999) to change the order of the remaining integral. Therefore,

$$\int_L^U \int_L^U s(y)(1-f_p(y)g(x,y)P(y,t_0)\mathrm{d}y\mathrm{d}x = \int_L^U \int_L^U s(y)(1-f_p(y)g(x,y)P(y,t_0)\mathrm{d}x\mathrm{d}y \tag{41}$$

$$= \int_L^U s(y)(1-f_p(y))P(y,t_0)\int_L^U g(x,y)\mathrm{d}x\mathrm{d}y \qquad (42)$$
$$= \int_L^U s(y)(1-f_p(y))P(y,t_0)\mathrm{d}y,$$

as $g(x,y)$ is a probability distribution for each fixed y. By the definition of $P(y,t_0)$, we see that the right-hand side of Eq. 42 equals $E_{n(\cdot,t_0)}(s(y)(1-f_p(y)))$. Finally, note that for every t, $\gamma(t)$ has the property that

$$\gamma(t) = \int_L^U c(y)n(y,t)\mathrm{d}y = \|n(\cdot,t)\|E_{n(\cdot,t)}(c(y)), \qquad (43)$$

which completes the proof.

Appendix 3: Notes on the Dirac Delta distribution

When used to model a structured population, the Dirac Delta distribution is the continuous-stage analog of a population vector that has zeros in all but one entry. In other words, the Dirac Delta distribution centered at a, written $\delta(x-a)$, roughly describes a population that is entirely of members whose stage variable equals a. Formally, $\delta(x-a)$ is the limit of a sequence of strongly peaked functions of the form:

$$\delta_n(x) = \begin{cases} 0 & for\, x < a - \dfrac{1}{2n} \\ n & for\, a - \dfrac{1}{2n} < x < a + \dfrac{1}{2n} \\ 0 & for\, x > a + \dfrac{1}{2n} \end{cases} \qquad (44)$$

as $n \to \infty$. $\delta(x-a)$ has the property that

$$\int_{-\infty}^{\infty} \phi(x)\delta(x-a)\mathrm{d}x = \phi(a) \qquad (45)$$

for all sufficiently smooth functions $\phi(x)$ (Logan 2006). More specifically, if one allows $\phi(x)=1$, then we see that $\delta(x-a)$ is a probability density function and

$$E_{\delta(x-a)}(\phi(x)) = \phi(a). \qquad (46)$$

References

Briggs J, Dabbs K, Riser-Espinoza D, Holm M, Lubben J, Rebarber R, Tenhumberg B (2010) Structured population dynamics and calculus: an introduction to integral modeling. Math Mag 83:243–257

Caswell H (2001) Matrix population models: construction, analysis and interpretation, 2nd edn. Springer, New York

Caswell H (2007) Sensitivity analysis of transient population dynamics. Ecol Lett 10:1–15

Caswell H (2008) Perturbation analysis of nonlinear matrix population models. Demogr Res 18:59–116

Cousens R (1991) Aspects of the design and interpretation of competition (inference) experiments. Weed Technol 5:664–673

R Development Core Team (2006) R: a language and environment for statistical computing. Vienna, Austria

Duncan RP, Diez JM, Sullivan JJ, Wangen S, Miller AL (2009) Safe sites, seed supply, and the recruitment function in plant populations. Ecology 90:2129–2138

Easterling MR, Ellner SP, Dixon PM (2000) Size-specific sensitivity: applying a new structured population model. Ecology 81:694–708

Ellner SP, Rees M (2006) Integral projection models for species with complex demography. Am Nat 167:410–428

Folland GB (1999) Real analysis: modern techniques and their applications. Wiley, New Jersey

Freckleton RP, Sutherland WJ, Watkinson AR, Stephens PA (2008) Modelling the effects of management on population dynamics: some lessons from annual weeds. J Appl Ecol 45:1050–1058

Hastings A (2004) Transients: the key to long-term ecological understanding? Trends Ecol Evol 19:39–45

Hinrichsen D, Pritchard AJ (2005) Mathematical systems theory I: modeling, state space analysis, stability and robustness. Springer, New York

Holling CS (1959) Some characteristics of simple types of predation and parasitism. Can Entomol 91:385–398

Koons DN, Grand JB, Zinner B, Rockwell RF (2005) Transient population dynamics: relations to life history and initial population state. Ecol Model 185:283–297

Logan JD (2006) Applied mathematics, 3rd edn. Wiley, New Jersey

Maki D, Thompson M (2006) Mathematical modeling and computer simulation. Thomson Brooks/Cole, Belmont

Mangel M (2006) The theoretical biologist's toolbox: quantitative methods for ecology and evolutionary biology. Cambridge University Press, Cambridge

Ramula S, Rees M, Buckley YM (2009) Integral projection models perform better for small demographic data sets than matrix population models: a case study of two perennial herbs. J Appl Ecol 46:1048–1053

Rebarber R, Tenhumberg B, Townley S (2011) Global asymptotic stability of density dependent integral projection models. Theor Pop Bio (in press)

Rose KE, Louda SM, Rees M (2005) Demographic and evolutionary impacts of native and invasive insect herbivores on *Cirsium canescens*. Ecology 86:453–465

Runge MC, Johnson FA (2002) The importance of functional form in optimal control solutions of problems in population dynamics. Ecology 83:1357–1371

Sletvold N (2002) Effects of plant size on reproductive output and offspring performance in the facultative biennial *Digitalis purpurea*. J Ecol 90:958–966

Snyder RE (2009) Transient dynamics in altered disturbance regimes: recovery may start quickly, then slow. Theor Ecol 2:79–87

Stott I, Franco M, Carslake D, Townley S, Hodgson D (2010) Boom or bust? A comparative analysis of transient population dynamics in plants. J Ecol 98:302–311

Tenhumberg B, Tyre TJ, Rebarber R (2009) Model complexity affects transient population dynamics following a dispersal event: a case study with pea aphids. Ecology 90:1878–1890

Townley S, Hodgson DJ (2008) Erratum et addendum: transient amplification and attenuation in stage-structured population dynamics. J Appl Ecol 45:1836–1839

Townley S, Carslake D, Kellie-Smith O, McCarthy D, Hodgson D (2007) Predicting transient amplification in perturbed ecological systems. J Appl Ecol 44:1243–1251

Vandermeer JH, Goldberg DE (2003) Population ecology: first principles. Princeton University Press, Princeton

Weiner J, Martinez S, Muller-Scharer H, Stoll P, Schmid B (1997) How important are environmental maternal effects in plants? A study with *Centaurea maculosa*. J Ecol 85:133–142

Weller M, Spratcher C (1965) Role of habitat in the distribution and abundance of marsh birds. Special report 43. Iowa Agriculture and Home Economics Experiment Station, Ames